Heliyon 11 (2025) e41436

Contents lists available at ScienceDirect

Heliyon

journal homepage: www.cell.com/heliyon

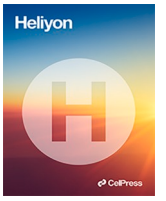

Research article

MSC-derived exosome ameliorates pulmonary fibrosis by modulating NOD 1/NLRP3-mediated epithelial-mesenchymal transition and inflammation

Wei Chen [a], Jie Peng [a], Xiangyi Tang [a], Shao Ouyang [b,*]

[a] Department of Respiratory and Critical Care Medicine, The Second Affiliated Hospital of University of South China, Hengyang, Hunan, China
[b] Department of Cardiovascular Medicine, The Second Affiliated Hospital of University of South China, Key Laboratory of Heart Failure Prevention & Treatment of Hengyang, Clinical Medicine Research Center of Arteriosclerotic Disease of Hunan Province, Hengyang, Hunan, China

ARTICLE INFO

Keywords:
Pulmonary fibrosis
MSC
Exosome
EMT
Inflammation
NLRP3

ABSTRACT

Background: Pulmonary fibrosis (PF) is an irreversible and usually fatal lung disease. In recent years, the therapeutic role of exosomes derived from mesenchymal stem cells (MSC-exos) in anti-fibrotic treatment has received much attention. In this study, we aimed to determine the anti-fibrotic properties and related molecular mechanisms of MSC-exos in Bleomycin(BLM)-induced PF.

Methods: We used BLM-induced mice model of PF and in vitro model. MSC-exos were isolated from BMSCs cells using Exo Quick-TC kit and identified using conventional methods. Using cell counting kit-8 (CCK-8) to detect cell viability. Classic molecular biology approaches such as RT-qPCR, Western blot, immunofluorescence, and ELISA were used to examine molecular pathways. Histopathological examination was performed using HE and Masson staining.

Results: MSC-exos alleviated inflammation, inhibited epithelial-mesenchymal transition (EMT), and ameliorated PF. Further studies showed that MSC-exos regulated NOD1/NF-kB signaling pathway to suppress the activation of NLRP3 inflammasomes both in vivo and in vitro. Additionally, overexpression of NLRP3 significantly reversed the anti-fibrotic effects of MSC-exos in BLM-induced lung epithelial cells.

Conclusion: MSC-derived exosome ameliorates pulmonary fibrosis by modulating NOD 1/NLRP3-mediated epithelial-mesenchymal transition and inflammation.

1. Introduction

Pulmonary fibrosis (PF) is a fatal, progressive, and chronic lung condition characterized by interstitial disease. It entails inflammation and substantial remodeling of the lungs due to the deposition of extracellular matrix (ECM). Consequently, widespread scar formation, respiratory failure, and eventual demise may ensue [1,2]. The lack of comprehensive insight into PF's pathogenesis hampers the development of effective clinical interventions. It was estimated that the diagnosed PF patients typically have a median survival of merely 3–5 years [3]. Hence, it is crucial to conduct thorough investigations into PF's pathogenesis and discover novel approaches for efficient clinical treatment.

Abbreviations: PF, Pulmonary fibrosis; ECM, Extracellular matrix; MSCs, Mesenchymal stem cells; NOD1, Domain-containing protein 1.

* Corresponding author.
E-mail address: ouyangshao2024@163.com (S. Ouyang).

https://doi.org/10.1016/j.heliyon.2024.e41436
Received 8 April 2024; Received in revised form 12 December 2024; Accepted 20 December 2024
Available online 26 December 2024

Mesenchymal stem cells (MSCs) are a type of versatile stem cells that possess the capability of self-renewal and diverse differentiation [4], exhibiting properties beneficial for biological processes such as reducing inflammation, moderating the immune response, promoting tissue repair, and mitigating fibrosis [4,5]. In the past decade, the potential therapeutic value of MSCs in lung afflictions has garnered considerable interest. Research findings indicate that MSCs have the ability to profoundly alleviate lung inflammation, impede epithelial-mesenchymal transition (EMT), and curtail lung tissue damage and fibrosis [6]. The growing evidences indicate that the predominant mechanism underlying the therapeutic effectiveness of MSCs is through paracrine activity, wherein exosomes derived from MSCs (MSC-exos) play a pivotal role as the principal paracrine constituents responsible for their biologically advantageous functions [7,8].The MSC-exos has the potential to alleviate the inflammation and collagen accumulation observed in idiopathic PF in mice, ultimately leading to an improvement in the condition [9]. Additionally, exosomal miR-466f-3p sourced from MSCs has demonstrated its ability to hinder the progression of PF by impeding the c-MET mediated AKT/GSK3β signaling pathway, effectively preventing radiation-induced EMT [10]. In summary, these findings highlight the promising therapeutic possibilities of MSC-exos in the treatment of PF.

The pathogenesis of PF is highly intricate and involves various factors, including inflammation, degradation of the ECM, EMT, and imbalanced deposition of collagen. NLRP3 serves as a prominent innate immune system sensor and represents the most distinctive and extensively implicated inflammasome in both acute and chronic lung diseases [11]. The activation of the NLRP3 inflammasome can hasten the onset and progression of PF [12,13]. Studies have shown that the NLRP3 inflammasome in alveolar epithelial cells may expedite the process of EMT through pathways such as TGF-β or NF-κB, ultimately leading to scar formation and collagen deposition in lung tissue, thereby exacerbating PF [14,15]. Research indicates that baicalin contributes to the improvement of PF by inhibiting NF-κB/NLRP3 mediated EMT and inflammation [14]. Additionally, the administration of NecroX-5 can mitigate inflammation, reduce oxidative stress, hinder EMT, and enhance the condition of PF by suppressing the NLRP3 inflammasome [16]. Consequently, inhibiting the activation of the NLRP3 inflammasome to suppress the EMT process and inflammatory response shows potential as a strategy to treat PF.

In our study, we found that decreased bleomycin (BLM)-induced inflammation, EMT, and PF in mice. Furthermore, our findings showed that MSC-exos reduce PF in vivo and in vitro via modulating the NOD1/NF-kB/NLRP3 pathway, which inhibits BLM-induced inflammation and EMT processes. This finding suggests a novel function for MSC-exos in PF.

2. Methods and materials

2.1. Animal

C57BL/6J mice, aged between 6 and 8 weeks, and weighing approximately 20 ± 2 g, were procured from the Experimental Animal Center at Hunan University of Traditional Chinese Medicine. The mice were accommodated in a meticulously regulated environment maintained at a constant temperature of 25 °C, relative humidity of 50 %, and a light-dark cycle of 12 h each. Adequate nutrition and purified water were available ad libitum. This animal experiment was approved by the Experimental Animal Ethics Review Committee of Guangzhou Seyotin Biotechnology Co., LTD (SYT2023036).

2.2. BLM-mediated PF in mice

Following a week of acclimatization, the mice underwent random allocation into three distinct experimental groups: control group, BLM group, and BLM + MSC-exos group(n = 3). A pulmonary fibrosis model was established based on previous reports [14]. The mice in the BLM group and BLM + MSC-exos group were anesthetized with 1 % pentobarbital sodium via intraperitoneal injection, and then 3 mg/kg of BLM (Zhejiang Hisun Pharmaceutical Co., Ltd., China) was intratracheally injected. The control group mice were intratracheally injected with an equal amount of sterile saline. Additionally, after the modeling was completed, the mice in the BLM + MSC-exos group were treated with 20 μg MSC-exos in 100 μL PBS via tail vein injection [17]. The mice were euthanized after a duration of 21 days. Their lung tissues were subsequently fixed in a solution of 4 % formaldehyde, embedded in paraffin, and subjected to both HE and Masson staining. The microscopic (Leica, Germany) was allowed for the observation of pathological alterations in the lung tissues.

2.3. Cell culture

The non-small cell lung cancer cells(A549) and BMSCs were obtained from Procell Life Science&Technology Co.,Ltd.(wuhan, China). They were cultured in RPMI1640 medium. The culture conditions included maintaining a stable CO2 level of 5 % and a temperature of 37 °C. To establish an in vitro injury model,1* 10^5 A549 cells were inoculated into the 24-well plate and stimulated with 50 μM BLM for 24 h [16].Then, cells were collected for follow-up detection after exosome (2 μg/mL) treatment.

2.4. Isolation of MSC-exos

MSC-exos were obtained from BMSCs through the utilization of the Exo Quick-TC kit (Precision Medicine Technology Co. Ltd, Beijing, China). In short, BMSCs were inoculated into T75 cell vials and replaced with exosom-free media when the cells had grown to 50%–70 %,the cell supernatant was collected after 48 h of culture.Then,the cell supernatant were underwent centrifugation at 3,000g for a duration of 15 min to eliminate cells and cellular debris. The resulting supernatant was moved to a sterile container and an

appropriate quantity of Exo Quick-TC (1:5) was added. The sample underwent gentle mixing and was subsequently incubated overnight at a temperature of 4 °C. Subsequently,The sample again was centrifuged at 1,500g for a duration of 30 min to obtained MSC-exos. Finally, the utilization of a transmission electron microscope (JSM-IT300, Japan) facilitated the observation of the morphological characteristics of MSC-exos.

2.5. Nanoparticle tracking analysis (NTA)

The exosomes were were diluted with TPM to a 1 mL volume. The size of exosomes was determined using a ZetaView PMX 110 (Particle Metrix, Meerbusch, Germany).

2.6. Cell proliferation assay

In order to evaluate the proliferation of A549 cells, A549 cells(5×10^3 cells) were inoculated in 96-well plates and incubated overnight at 37 °C. A549 cells were stimulated with 50 μM BLM for 24 h, and then treated with MSC-exos for 24 h.Next, 10 μL CCK-8 solution was added to each well and incubated at 37 °C for 2 h. The absorbance was measured at 450 nm.

2.7. RT-qPCR

The extraction of total RNA from lung tissues and A549 cells was performed using TriPure reagent (BioTeke Bio., Beijing, China) following the guidelines provided by the manufacturer. Subsequently, the obtained RNA underwent reverse transcription into cDNA employing the BeyoRT™ II M-MLV reverse transcription kit (Beyotime Biotechnology, Shanghai, China). In the end, the synthesized cDNA underwent RT-qPCR reaction utilizing Takara's sybr premix ex taq 2 kits from Japan. The genes primers sequences in Table 1. The $2^{-\Delta\Delta CT}$ method was employed to analyze the relative expression levels of the desired genes, with GAPDH serving as the reference gene.

2.8. Western blot

The proteins were obtained from lung tissues and A549 cells, and the concentration of protein was evaluated using the BCA assay kit (Beyotime Biotechnology, Shanghai). SDS-PAGE was utilized to separate the desired proteins, which were subsequently transferred onto a PVDF membrane. To prevent non-specific binding, the membrane was treated with 5 % skim milk for 2 h, followed by incubation with primary antibodies, MMP2 (A6247,abclonal, Wuhan, China), MMP9 (A0289,abclonal, Wuhan, China), N-cadherin (A0432,abclonal, Wuhan, China), snail (A24806,abclonal, Wuhan, China), vimentin (ab92547,abcam, shanghai, China), fibronectin (A12977, abclonal,Wuhan, China), E-cadherin (A3044, abclonal, Wuhan, China), NOD1 (A1246,abclonal, Wuhan, China), p-p65 (AP1294, abclonal, Wuhan, China), p65 (80979-1-RR,proteintech, Wuhan, China), NLRP3 (A5652,abclonal, Wuhan, China), Caspase1 (A23429, abclonal, Wuhan, China), caspase11 (A16792,abclonal, Wuhan, China), ASC (A1170,abclonal, Wuhan, China), IL-1beta (A16288,abclonal, Wuhan, China), IL-18 (A1115,abclonal, Wuhan, China), CD9 (A19027,abclonal, Wuhan, China), CD63 (A19023, abclonal, Wuhan, China), TSG-101(A2216,abclonal, Wuhan, China), and GAPDH (60004-1-Ig,Proteintech, Wuhan, China) overnight at 4 °C. Following a 1-h incubation with secondary antibodies at room temperature, the SuperSignal™ chemiluminescent substrate was implemented to visualize the protein bands (Thermo Fisher Scientific, Shanghai, China).

Table 1
Primer sequences.

Genes	Forward(5′-3′)	Reverse(5′-3′)
IL-1β	AGCTGAAAGCTCTCCACCTC	TGGGTGTGCCGTCTTTCATT
IL-18	ACTTTGGCCGACTTCACTGT	CAGTCTGGTCTGGGGTTCAC
NLRP3	CCAGGAGGACAGCCTTGAAG	GCGCGTTCCTGTCCTTGATA
NOD1	TGGCCCTAGACCTGGACAAC	ACCCAGGAACGTCACGATCT
Caspase1	GGACTGACTGGGACCCTCAA	GCTCCAACCCTCGGAGAAAG
Caspase11	TCTCACTGAGGTATGGGGCT	TGGTGTTCTGAGAGTGCAGC
ASC	CGTATGGCTTGGAGCTCACA	TGCTGGTCCACAAAGTGTCC
MMP2	CAACGGTCGGGAATACAGCA	GCTGTCCATCTGCATTGCCA
MMP9	GGTGTAGCACAACAGCTGAC	AGTGGTGCAGGCAGAGTAGG
N-cadherin	GCTCAGGACCCCGATCGATA	AGGCGGGATTCCATTGTCAG
E-cadherin	TTGAGAGGGAGACAGGCTGG	TCTCCATGGGATCCTCCACC
snail	CACACGCTGCCTTGTGTCTG	GGTTGGAGCGGTCAGCAAAA
vimentin	GCACGTCTTGACCTTGAACG	AGGCTTGGAAACGTCCACAT
fibronectin	GCACCACCCAGAACTACGAT	GCCCAGGTCATGCTGCTTAT
α-SMA	CTTCAATGTCCCCGCCATGT	GCCCTCATAGATAGGCACGT
Co1-I	CTTCAGGGAATGCCTGGTGA	ACCACTGGGACCAGCTTCAC
GAPDH	CCTGCACCACCAACTGCTTA	ATCACGCCACAGCTTTCCAG

2.9. ELISA

The expression of IL-1beta and IL-18 was detected using the IL-1beta ELISA Kit (ab214025, abcam, Shanghai, China) and IL-18 ELISA Kit (ab215539, abcam, Shanghai, China), respectively. Each experiment was repeated at least three times.

2.10. Statistical analysis

The utilization of GraphPad Prism software facilitated the execution of statistical analysis, wherein the outcomes were denoted as mean ± SD. To compare between different groups, the intergroup comparisons were performed by employing one-way ANOVA. Significantly distinct differences were considered when $P < 0.05$.

3. Result

3.1. Isolation and Identification of MSC-exos

The exosome isolation reagent kit to extract MSC-exos from BMSCs cells. The intact exosome membrane structures, exhibiting the characteristic cup-shaped morphology, were observed through transmission electron microscopy (Fig. 1A). Nano-particle tracking displayed diameters ranging from 100 to 1000 nm for the obtained MSC-exos (Fig. 1B). Protein imprinting technique confirmed the presence of common exosome markers, among them CD63, TSG101, CD9 and Calnexin, in MSC-exos (Fig. 1C). Consequently, these findings establish the successful isolation of MSC-exos from stem cells.

3.2. MSC-exos alleviate BLM-induced PF progression

MSCs are a type of multipotent stem cells with biological characteristics such as anti-inflammatory, immunomodulatory, and antifibrotic effects [4,5]. In recent years, the therapeutic effects of MSC-exos in lung injury diseases through paracrine pathways have attracted attention [17]. To investigate the role of MSC-exos in fibrosis, mice were induced with BLM to induce PF. Compared to the control group, PF mice exhibited significantly thickened alveolar walls and inflammatory infiltration. The PF mice treated with MSC-exos significantly alleviated the fibrotic symptoms (Fig. 2A). Masson's staining revealed the formation of significant blue-stained fibrous strands and collagen deposition in the lung tissues of fibrotic mice. However, this condition was significantly reversed in the lung tissues of fibrotic mice treated with MSC-exos, reducing collagen deposition in the lung tissues (Fig. 2B). Subsequently, RT-qPCR was used to measure the mRNA levels of fibrotic biomarkers α-SMA and Co1-I, as shown in Fig. 2C. The expression of α-SMA and Co1-I

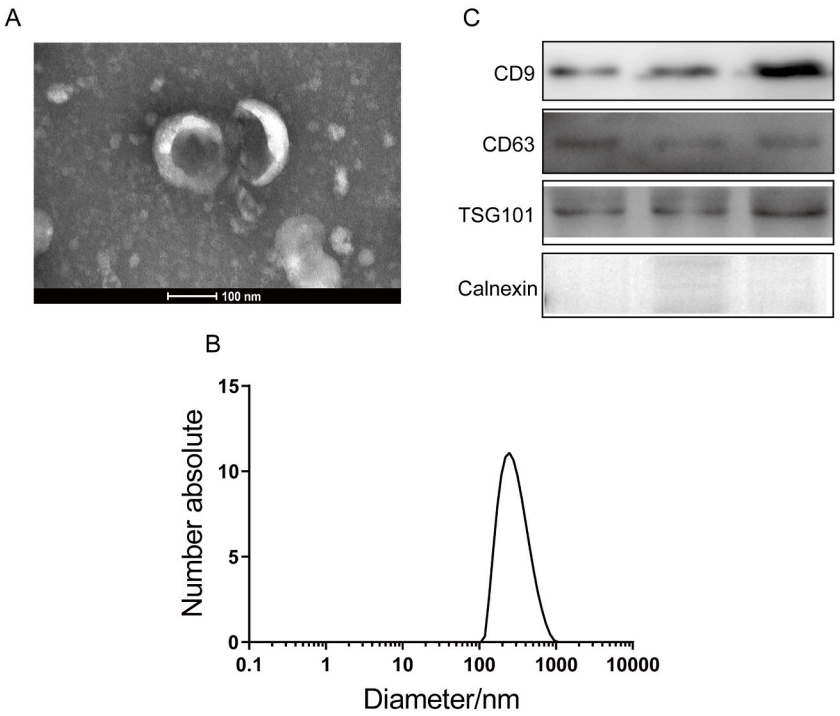

Fig. 1. Isolation and Identification of MSC-exos. A. Transmission electron microscopy observation of exosomes. B. Exosome size analysis. C. Protein imprint detection of CD9, CD63, TSG-101 expression.

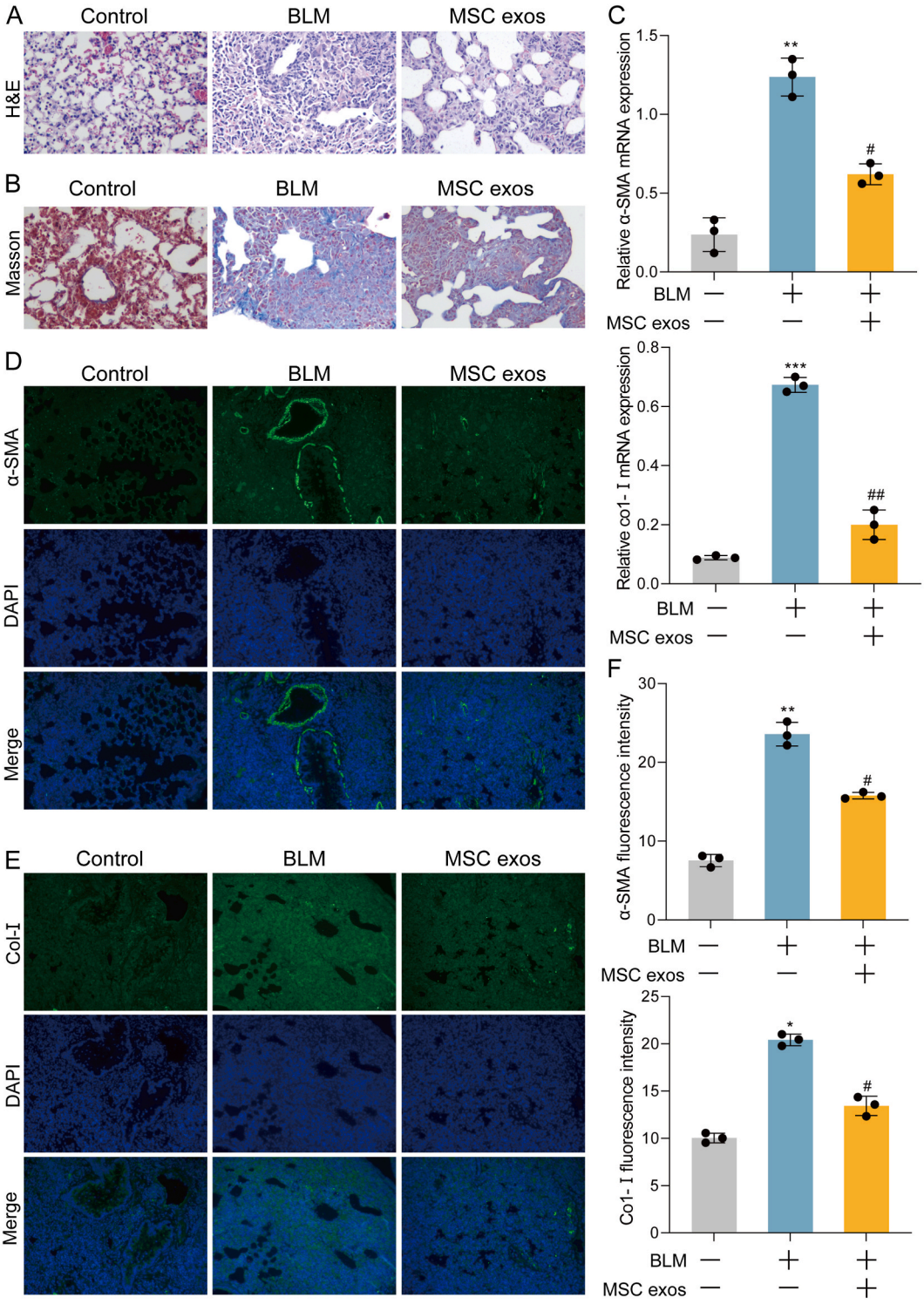

Fig. 2. MSC-exos alleviate BLM-induced PF progression. A. HE staining evaluation of mouse lung tissue pathology. B. Masson staining evaluation of lung tissue pathology. C. RT-qPCR detection of α-SMA and Co1-I expression in mouse lung tissue. D-E. Immunofluorescence detection of α-SMA and Co1-I in mouse lung tissue. F. Quantification of immunofluorescence images of α-SMA and Co1-I. n = 3; *P < 0.05, **P < 0.01vs Control group, #P < 0.05, ##P < 0.01 vs BLM group.

was upregulated in BLM-induced PF mice, but the expression was decreased in PF mice treated with MSC-exos (Fig. 2C). In addition, immunofluorescence experiments showed a similar change in the levels of α-SMA and Co1-I mRNA. The expression levels of α-SMA (Fig. 2D) F and Co1-I(Fig. 2E and F) were significantly reduced in the lung tissues of PF mice treated with MSC-exos. These results indicate that MSC-exos significantly improve the progression of BLM-induced PF in mice.

3.3. MSC-exos inhibit EMT process in BLM-induced mouse PF model

The process of EMT is a crucial factor contributing to fibrosis [18]. EMT plays a role in the pathogenesis of fibrotic diseases, including lung fibrosis, kidney fibrosis, and liver fibrosis [19]. In this study, we aimed to investigate the impact of MSC-exos on the occurrence of EMT in a mouse model of pulmonary fibrosis induced by BLM. The RT-qPCR analysis revealed an upregulation in the mRNA levels of fibronectin, vimentin, N-cadherin, MMP-2, MMP-9, and Snail, along with a downregulation in the mRNA levels of E-cadherin in the lung tissues of BLM-induced pulmonary fibrosis mice (Fig. 3A), indicating the presence of EMT during BLM-induced pulmonary fibrosis. However, the lung tissues of PF mice treated with MSC-exos exhibited a noticeable reversal in this trend.

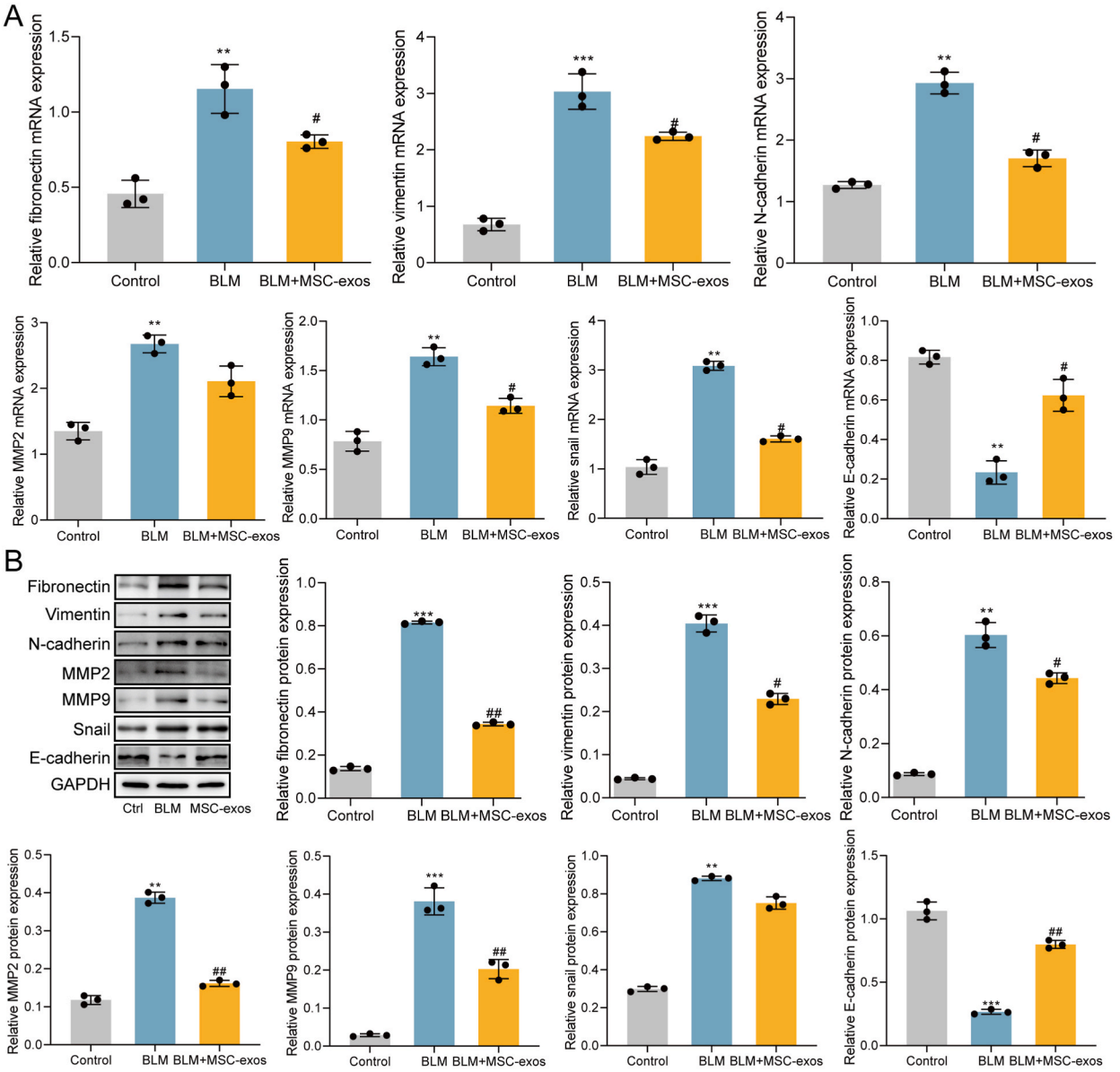

Fig. 3. MSC-exos inhibit EMT process in BLM-induced PF model. A. RT-qPCR detection of MMP2, MMP9, N-cadherin, snail, vimentin, fibronectin, and E-cadherin expression in mouse lung tissue. B. Protein imprint detection of MMP2, MMP9, N-cadherin, snail, vimentin, fibronectin, and E-cadherin expression in mouse lung tissue.n = 3; $^{**}P < 0.01$, $^{***}P < 0.001$ vs Control group, $^{\#}P < 0.05$, $^{\#\#}P < 0.01$ vs BLM group.

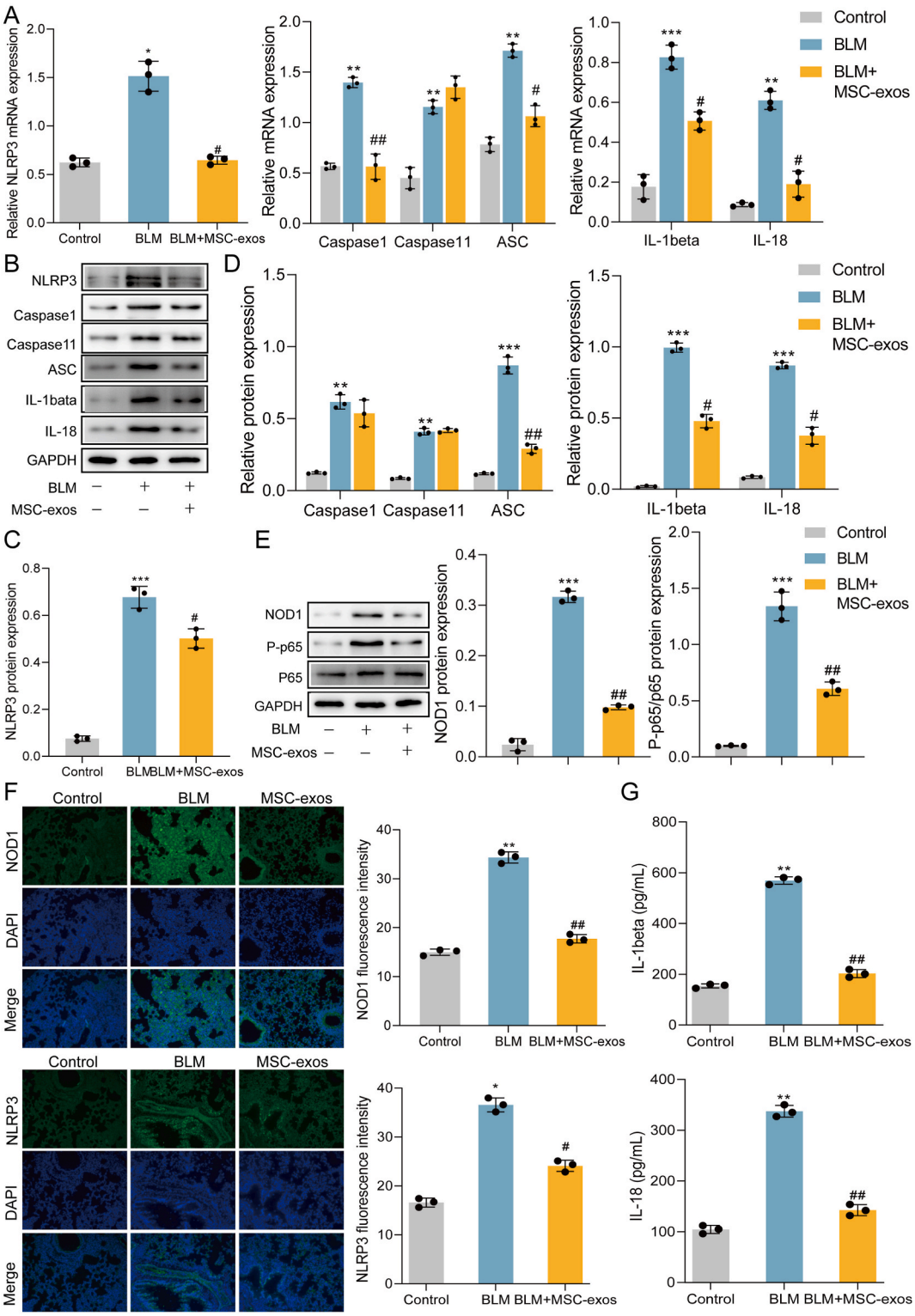

Fig. 4. MSC-exos suppress inflammation in the BLM-induced PF model by regulating the NOD1/NF-κB/NLRP3 pathway. A. RT-qPCR detection of NLRP3, NOD1, Caspase1, caspase11, ASC, IL-1beta, IL-18 expression in lung tissue. B. Protein imprint detection of NLRP3, Caspase1, caspase11, ASC, IL-1beta, IL-18 expression in lung tissue. C-D. Quantification of protein imprint results using image J. E. Protein imprint detection of NOD1, p-p65, and p65 expression in lung tissue. F. Immunofluorescence detection of NOD1, NLRP3 expression in lung tissue. G. ELISA analysis of IL-1beta, IL-18 content in serum. n = 3; *P < 0.05, **P < 0.01, ***P < 0.001 vs Control group, #P < 0.05, ##P < 0.01 vs BLM group.

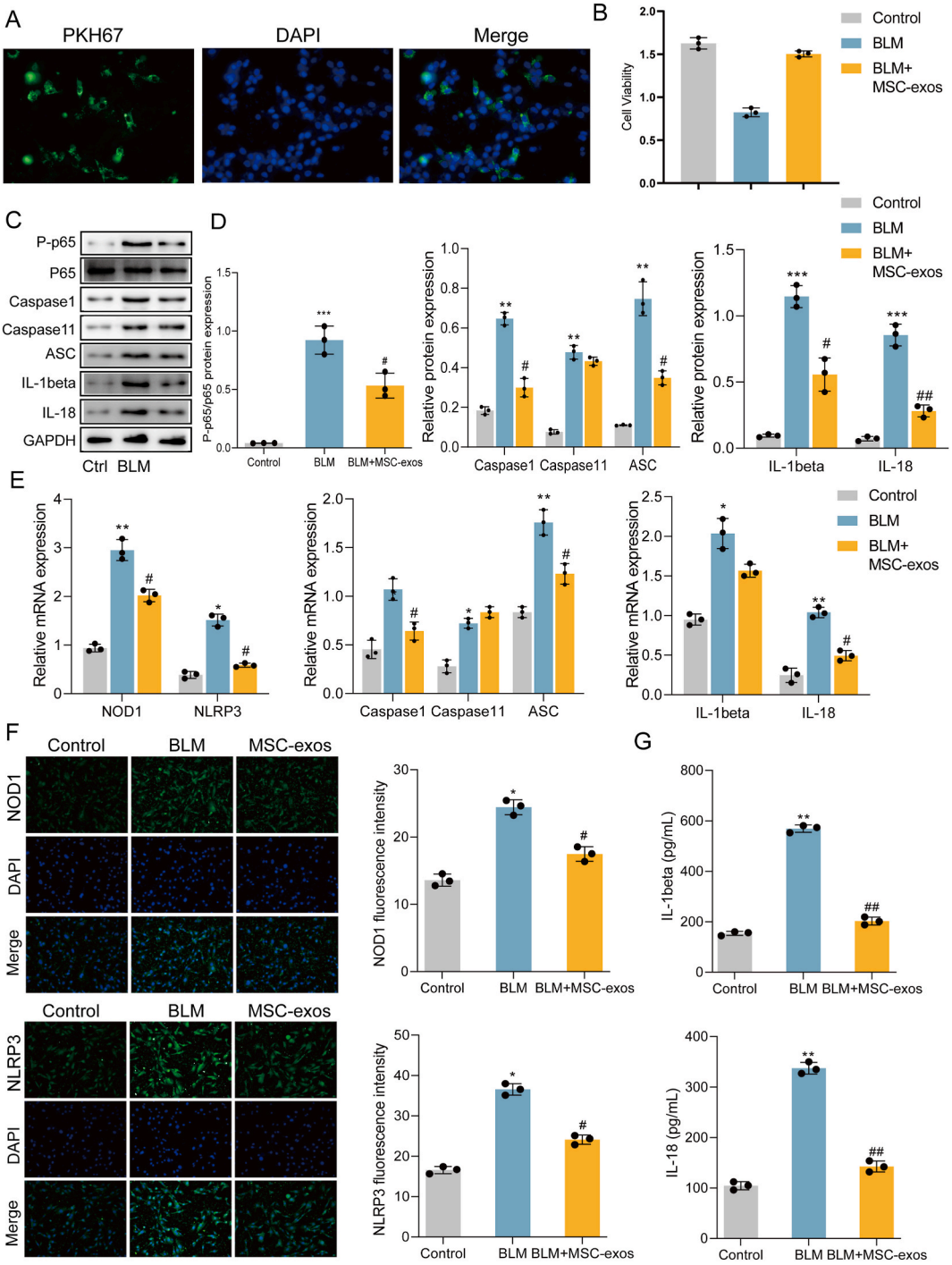

Fig. 5. MSC-exos inhibit BLM-induced inflammation through the NOD1/NF-κB/NLRP3 pathway in vitro. A. Immunofluorescence tracking of A549 cells' uptake of exosomes. B.Cell viability was measured by CCK8. C. Protein imprint detection of p-p65, p65, Caspase1, caspase11, ASC, IL-1beta, IL-18 expression in A549 cells. D. Quantification of protein imprint results using image J. E. RT-qPCR detection of NLRP3, NOD1, Caspase1, caspase11, ASC, IL-1beta, IL-18 expression in A549 cells. F. Immunofluorescence detection of NOD1, NLRP3 expression in A549 cells. G. ELISA analysis of IL-1beta, IL-18 content in cell supernatant.n = 3; *P < 0.05, **P < 0.01, ***P < 0.001 vs Control group, #P < 0.05, ##P < 0.01 vs BLM group.

Specifically, the mRNA levels of fibronectin, vimentin, N-cadherin, MMP-2, MMP-9, and Snail decreased, while the mRNA levels of E-cadherin increased (Fig. 3A). Western blot analysis further confirmed these findings, as the protein levels of fibronectin, vimentin, N-cadherin, MMP-2, MMP-9, and Snail were elevated in the BLM group, whereas E-cadherin protein expression was diminished. Conversely, in the MSC-exos group, the expression levels of fibronectin, vimentin, N-cadherin, MMP-2, MMP-9, and Snail decreased, while E-cadherin protein expression increased (Fig. 3B). These results provide evidence that MSC-exos effectively inhibit the EMT process in a mice model of BLM-induced PF.

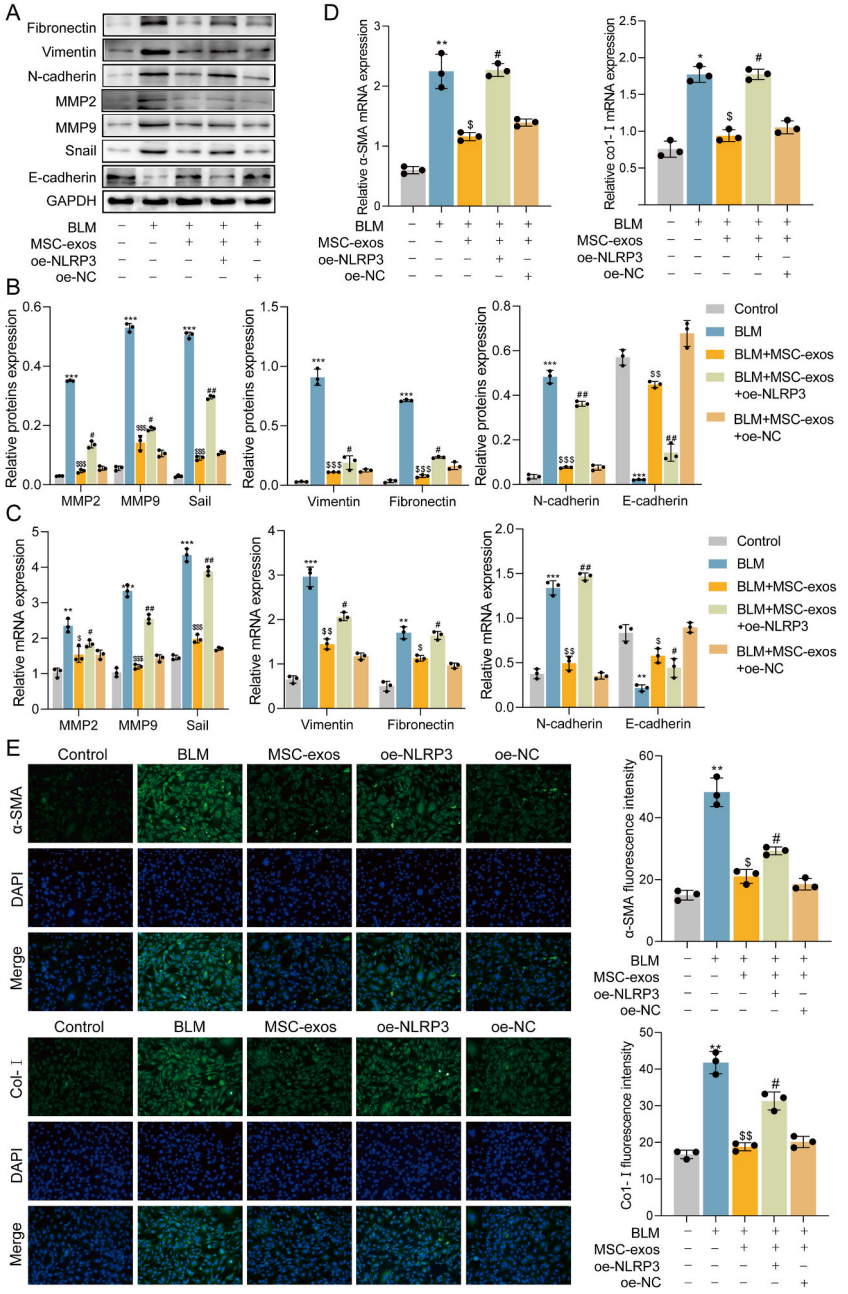

Fig. 6. Overexpression of NLRP3 reverses the effects of MSC-exos on BLM-induced EMT and extracellular matrix deposition in vitro. A. Protein imprint detection of MMP2, MMP9, N-cadherin, snail, vimentin, fibronectin, and E-cadherin expression. B. Quantification of protein imprint results using image J. C. RT-qPCR detection of MMP2, MMP9, N-cadherin, snail, vimentin, fibronectin, and E-cadherin. D. RT-qPCR detection of α-SMA and Co1-I expression in A549 cells. E. Immunofluorescence detection of α-SMA and Co1-I expression in A549 cells. n = 3; *P < 0.05, **P < 0.01, ***P < 0.001 vs Control group, $P < 0.05, $$P < 0.01, $$$P < 0.001 vs BLM group, #P < 0.05, ##P < 0.01 vs BLM + MSC-exos group.

3.4. MSC-exos suppress inflammation in the BLM-induced PF model by regulating the NOD1/NF-κB/NLRP3 pathway

The role of excessive inflammatory response is crucial in the onset of PF [20]. Hence, our study aimed at exploring the impact of MSC-exos on lung inflammation in PF mice by modulating NLRP3 inflammasome. RT-qPCR results showed upregulation of NLRP3 inflammasome activation in BLM-induced PF mice, with an upregulation in the mRNA expression levels of NLRP3, caspase-1, caspase-11, ASC, IL-1beta, and IL-18. In contrast, the mRNA expression levels of caspase-11, NLRP3, caspase-1, ASC, IL-1beta, and IL-18 were decreased in the lung tissues of PF mice treated with MSC-exos (Fig. 4A). Western blotting results showed that the protein levels of NLRP3, caspase-1, caspase-11, ASC, IL-1beta, and IL-18 were increased in the BLM group, while the levels were significantly decreased in the lung tissues of PF mice treated with MSC-exos, except for caspase-11 (Fig. 4B–D). These results demonstrate that MSC-exos suppress inflammation in BLM-induced mouse PF model by inhibiting the activation of the NLRP3 inflammasome. NOD1, which belongs to the cytoplasmic NOD-like receptor (NLR) family, has the ability to activate NF-κB and trigger inflammation [21]. It is well-known that the activation of the NF-κB signaling pathway plays a crucial role in the activation of the NLRP3 inflammasome [22]. Thus, we hypothesized that MSC-exos might hinder the activation of the NLRP3 inflammasome through the NOD1/NF-κB pathway. As anticipated, the findings from the protein imprinting experiments demonstrated a significant upregulation of NOD1 expression in BLM-induced PF mice, alongside an increased ratio of phosphorylated p65 to total p65 (p-p65/p65). Conversely, the protein levels of NOD1 and the p-p65/p65 ratio were reduced in the lung tissues of PF mice that were treated with MSC-exos (Fig. 4E). Immunofluorescence also confirmed these results, with significant upregulation of NOD1 and NLRP3 levels in the lung tissues of BLM-induced PF mice, while the levels were significantly decreased in the lung tissues of PF mice treated with MSC-exos (Fig. 4F). Additionally, ELISA results showed that the levels of IL-1beta and IL-18 in the serum of BLM-induced PF mice were significantly increased, while the levels were significantly decreased in the lungs of PF mice treated with MSC-exos (Fig. 4G). Overall, our experimental results demonstrate that MSC-exos suppress inflammation in the BLM-induced mouse PF model by regulating the NOD1/NF-κB/NLRP3 pathway.

3.5. MSC-exos inhibit BLM-induced inflammation through the NOD1/NF-κB/NLRP3 pathway in vitro

We conducted further investigations to determine the potential impact of MSC-exos on BLM-induced inflammation via the NOD1/NF-κB/NLRP3 pathway in vitro. The co-culture experiment involving A549 cells and MSC-exos was conducted, and in Fig. 5A revealed successful uptake of MSC-exos by A549 cells. To assess the growth rate of A549 cells, the CCK-8 assay was employed to viability. Notably, the result in Fig. 5B indicate that MSC-exosomes enhanced cell viability. Following this, RT-qPCR and Western blotting were employed to verify the activation NOD1/NF-κB/NLRP3 pathway in the BLM-stimulated cell model, show casing an increase in the expression levels of NOD1, p-p65/p65, NLRP3, caspase-1, caspase-11, ASC, IL-1beta, and IL-18 in A549 cells. Remarkably, the treatment of MSC-exos to A549 cells demonstrated a reversal of these effects (Fig. 5C–E). Furthermore, immunofluorescence staining experiments exhibited heightened NOD1 and NLRP3 levels in BLM-induced A549 cells. In contrast, treatment with MSC-exos significantly diminished the expression levels of both NOD1 and NLRP3 (Fig. 5F). Additionally, ELISA results indicated an increase in the concentrations of IL-1beta and IL-18 in the supernatant of BLM-treated A549 cells. However, the treatment with MSC-exos led to a significant reduction in the levels of IL-1beta and IL-18 within the supernatant (Fig. 5G). Collectively, these findings suggest that MSC-exos effectively inhibit BLM-induced inflammation through the NOD1/NF-κB/NLRP3 pathway in vitro.

3.6. Overexpression of NLRP3 reverses the effects of MSC-exos on BLM-induced EMT and extracellular matrix deposition in vitro

To examine the crucial role played by the NLRP3 inflammasome in the antifibrotic effects of MSC-exos, we decided to boost NLRP3 expression in A549 cells. The outcomes of both Western blotting and RT-qPCR analyses revealed that the overexpression of NLRP3 (OE-NLRP3) counteracted the inhibitory impact exerted by MSC-exos on EMT. Specifically, we observed an upregulation in the expression levels of MMP2, MMP9, N-cadherin, snail, vimentin, and fibronectin, while the expression of E-cadherin was downregulated within the A549 cells (Fig. 6A–C). Additionally, through RT-qPCR analysis, OE-NLRP3 a significant increase in the expression of α-SMA and Co1-I within A549 cells that had been treated with MSC-exos and simultaneously OE-NLRP3 (Fig. 6D). This finding was further verified via immunofluorescence staining, which exhibited a pronounced elevation in the expression levels of α-SMA and Co1-I within A549 cells that had been treated with MSC-exos and OE-NLRP3 (Fig. 6E). Collectively, these experimental findings provide solid evidence that the overexpression of NLRP3 can reverse the influence of MSC-exos on EMT and the deposition of extracellular matrix components in vitro.

4. Discussion

PF is an incurable, progressive interstitial lung disease with a bad prognosis and few treatment options [23]. Consequently, there is an urgent need to investigate prospective targets and novel treatment strategies for PF in the clinical setting. Recent studies have extensively examined the therapeutic potential of MSC-exos in various lung diseases. For instance, exosomes obtained from human embryonic stem cells have been found to deter PF by targeting thrombospondin-2 [24]. Similarly, exosomes derived from human umbilical cord mesenchymal stem cells have demonstrated alleviating effects on PF in mice by inhibiting EMT [25]. The aim of our study was to isolate exosomes from HUCMSCs and investigate the role they play, as well as the molecular mechanisms involved, in PF. Our findings highlight that MSC-exos possess inhibitory properties against BLM-induced PF, both in vivo and in vitro. These MSC-exos effectively reduce the levels of α-SMA and CoL-I, leading to an improvement in collagen deposition within the fibrotic model induced by BLM. Furthermore, we provide evidence demonstrating that MSC-exos alleviate PF by restraining the EMT process through the

NOD1/NLRP3 pathway in vivo and in vitro.

Increasing evidence suggests that the EMT process is a key initiator and contributor in PF [26,27]. In the progression of PF, epithelial cells lose epithelial adhesion proteins such as E-cadherin, accompanied by the acquisition of mesenchymal cell markers, including N-cadherin and α-SMA in mesenchymal cells [28,29]. Our results suggest that EMT contributes to the pathogenesis of PF, which is consistent with previous studies [16]. Furthermore, we found that MSC-exos inhibit BLM-induced EMT both in vivo and in vitro, reducing the expression levels of EMT markers such as Fibronectin, Vimentin, N-cadherin, MMP-2, MMP-9, and Snail at the protein and mRNA levels, and upregulating the expression of E-cadherin, revealing the improvement of PF through the inhibition of EMT by MSC-exos.

Imbalanced inflammation also contributes to the development of PF according to previous research [20]. Inflammasomes play a crucial role in regulating inflammation and fibrosis in the lungs, with NLRP3 being the most notable inflammasome [30,31]. Although the activation of NLRP3 inflammasomes has been confirmed to promote the progression of PF, the underlying mechanisms remain not fully understood. Specifically, when the inflammatory sensor recognizes patterns associated with pathogens (PAMPs) or damage (DAMPs), it triggers the activation of the NF-κB signaling pathway. Consequently, there is an increase in the expression of components related to inflammasomes (e.g., NLRP3, pro-IL-1β, and pro-IL-18) at the transcriptional level. Subsequently, the adapter protein ASC is recruited to NLRP3, facilitating its interaction with caspase-1 and leading to caspase-1 activation. The active caspase-1 can then facilitate the maturation of pro-inflammatory cytokines IL-1β and IL-18 [32,33]. Additionally, the non-canonical caspase-11 inflammasome pathway can also promote the maturation and secretion of IL-1β by triggering the activation of the classical NLRP3 inflammasome [34]. Our study consistently detected upregulation of NLRP3, Caspase1, Caspase11, ASC, IL-1β, and IL-18 in the BLM-induced lung fibrotic model. Importantly, we observed that MSC-exos can inhibit the activation of the NLRP3 inflammasome and alleviate inflammation in PF by regulating caspase-1 rather than caspase-11, which aligns with previous findings [16].

Nucleotide-binding oligomerization domain-containing protein 1 (NOD1) is a member of the NLR family and is a cytoplasmic innate immune receptor that drives innate immune responses and triggers a series of inflammatory signaling events upon sensing pathogens or tissue damage [35]. Early studies have shown that NOD1 and NOD2 mediate the activation of the transcriptional regulatory factor nuclear factor kappa B (NF-κB), known to be upstream of NLRP3. Previous studies have reported that NOD1 enhances and induces NLRP3 inflammasome activation [36,37]. In this study, we found that BLM-induced PF model promotes NOD1 signaling, NF-κB p65 phosphorylation, and subsequently induces NLRP3 inflammasome activation, which is consistent with previous reports [37]. Interestingly, we also found that MSC-exos significantly inhibit NOD1 and NF-κB p65 phosphorylation in the BLM-induced PF model. Therefore, our experimental results suggest that MSC-exos may inhibit NLRP3 inflammasome activation through the NOD1/NF-κB pathway.

In addition, several studies have reported that NLRP3 inflammasome activation accelerates EMT in the progression of PF [38,39]. Therefore, we hypothesize that MSC-exos alleviate BLM-induced PF by inhibiting NLRP3 inflammasome activation and subsequently suppressing the EMT process. We upregulated the expression of NLRP3 in A549 cells and found that OE-NLRP3 abolished the inhibitory effect of MSC-exos on EMT and promoted fibrosis in A549 cells. This experimental result suggests that MSC-exos improve BLM-induced PF by inhibiting the EMT process, which depends on the inhibition of NLRP3 inflammasome.Based on our research, it is evident for the very first time that MSC-exos possess the capability to impede the activation of NLRP3 inflammasome by acting on the NOD1/NF-κB pathway. This action leads to the inhibition of inflammation as well as the EMT process, ultimately resulting in the amelioration of PF advancement.

Our study shows the potential of MSC-exos in the treatment of PF, but there are still many challenges in translating these findings into clinical application. First, we need to isolate MSC-exos on the scale of GMP and ensure that the quality and biological activity of MSC-exos meet the requirements of GMP production. Secondly, we need to conduct strict preclinical and clinical trials to verify the safety and effectiveness.

5. Conclusions

Our study conclusively confirms the therapeutic potential of MSC-exos in attenuating the progression of pulmonary fibrosis. Furthermore, we have discussed the underlying mechanisms, offering a promising strategy for the clinical treatment of PF.

CRediT authorship contribution statement

Wei Chen: Funding acquisition, Data curation, Conceptualization. **Jie Peng:** Methodology, Investigation, Data curation. **Xiangyi Tang:** Methodology, Investigation, Data curation. **Shao Ouyang:** Writing – review & editing, Writing – original draft, Funding acquisition, Data curation, Conceptualization.

Availability of data and materials

For inquiries regarding the availability of data and materials, please reach out to the corresponding author.

Ethics approval and consent to participate

All experiments were approved by the Experimental Animal Ethics Review Committee of Guangzhou Seyotin Biotechnology Co., LTD (SYT2023036).

Human ethics

Not Applicable.

Consent for publication

All authors Consent for publication.

Funding

This research was supported by the Hunan Provincial Science and Health Joint Fund (No.2021JJ70110), the clinical medical technology innovation guide project of Hunan Province(2021SK51712), the Key Scientific Research Project of Department of Education of Hunan Province (23A0318).

Declaration of competing interest

The authors declare the following financial interests/personal relationships which may be considered as potential competing interests:Chen reports financial support was provided by The Second Affiliated Hospital of the University of South China. Reports a relationship with that includes:. Has patent pending to. If there are other authors, they declare that they have no known competing financial interests or personal relationships that could have appeared to influence the work reported in this paper.

Acknowledgment

we are very grateful to Guangzhou Seyotin Biotechnology Co., Ltd. for their guidance and help in animal experiments. Dr. Xuan helped us revise the manuscript and submit the paper together.

Appendix A. Supplementary data

Supplementary data to this article can be found online at https://doi.org/10.1016/j.heliyon.2024.e41436.

References

[1] L. Tanner, A.B. Single, R.K.V. Bhongir, et al., Small-molecule-mediated OGG1 inhibition attenuates pulmonary inflammation and lung fibrosis in a murine lung fibrosis model, Nat. Commun. 14 (1) (2023) 643.
[2] N.N. Dsouza, V. Alampady, K. Baby, et al., Thalidomide interaction with inflammation in idiopathic pulmonary fibrosis, Inflammopharmacology 31 (3) (2023) 1167–1182.
[3] T. Yanagihara, S.G. Chong, M. Vierhout, et al., Current models of pulmonary fibrosis for future drug discovery efforts, Expet Opin. Drug Discov. 15 (8) (2020) 931–941.
[4] L. Hou, Z. Zhu, F. Jiang, et al., Human umbilical cord mesenchymal stem cell-derived extracellular vesicles alleviated silica induced lung inflammation and fibrosis in mice via circPWWP2A/miR-223-3p/NLRP3 axis, Ecotoxicology and environmental safety 251 (2023) 114537.
[5] Y. Yang, Y. Chen, Y. Liu, et al., Mesenchymal stem cells and pulmonary fibrosis: a bibliometric and visualization analysis of literature published between 2002 and 2021, Front. Pharmacol. 14 (2023) 1136761.
[6] T.A. Wynn, Cellular and molecular mechanisms of fibrosis, J. Pathol. 214 (2) (2008) 199–210.
[7] S. Ren, Y. Lin, W. Liu, et al., MSC-Exos: important active factor of bone regeneration, Front. Bioeng. Biotechnol. 11 (2023) 1136453.
[8] M. Guo, Z. Yin, F. Chen, et al., Mesenchymal stem cell-derived exosome: a promising alternative in the therapy of Alzheimer's disease, Alzheimer's Res. Ther. 12 (1) (2020) 109.
[9] M. Choi, T. Ban, T. Rhim, Therapeutic use of stem cell transplantation for cell replacement or cytoprotective effect of microvesicle released from mesenchymal stem cell, Mol. Cell. 37 (2) (2014) 133–139.
[10] Y. Li, Z. Shen, X. Jiang, et al., Mouse mesenchymal stem cell-derived exosomal miR-466f-3p reverses EMT process through inhibiting AKT/GSK3β pathway via c-MET in radiation-induced lung injury, Journal of experimental & clinical cancer research: CR 41 (1) (2022) 128.
[11] R. Fusco, R. Siracusa, T. Genovese, et al., Focus on the role of NLRP3 inflammasome in diseases, Int. J. Mol. Sci. 21 (12) (2020).
[12] J.W. Pinkerton, R.Y. Kim, A.A.B. Robertson, et al., Inflammasomes in the lung, Mol. Immunol. 86 (2017) 44–55.
[13] M. Biasizzo, N. Kopitar-Jerala, Interplay between NLRP3 inflammasome and autophagy, Front. Immunol. 11 (2020) 591803.
[14] L. Peng, L. Wen, Q.F. Shi, et al., Scutellarin ameliorates pulmonary fibrosis through inhibiting NF-κB/NLRP3-mediated epithelial-mesenchymal transition and inflammation, Cell Death Dis. 11 (11) (2020) 978.
[15] R. Tian, Y. Zhu, J. Yao, et al., NLRP3 participates in the regulation of EMT in bleomycin-induced pulmonary fibrosis, Experimental cell research 357 (2) (2017) 328–334.
[16] L. Min, Z. Shu-Li, Y. Feng, et al., NecroX-5 ameliorates bleomycin-induced pulmonary fibrosis via inhibiting NLRP3-mediated epithelial-mesenchymal transition, Respiratory research 23 (1) (2022) 128.
[17] N. Mansouri, G.R. Willis, A. Fernandez-Gonzalez, et al., Mesenchymal stromal cell exosomes prevent and revert experimental pulmonary fibrosis through modulation of monocyte phenotypes, JCI insight 4 (21) (2019).
[18] Y. Ishida, Y. Kuninaka, N. Mukaida, et al., Immune mechanisms of pulmonary fibrosis with bleomycin, Int. J. Mol. Sci. 24 (4) (2023).
[19] G.D. Marconi, L. Fonticoli, T.S. Rajan, et al., Epithelial-mesenchymal transition (EMT): the type-2 EMT in wound healing, tissue regeneration and organ fibrosis, Cells 10 (7) (2021).
[20] M. Yang, D. Wang, S. Gan, et al., Triiodothyronine ameliorates silica-induced pulmonary inflammation and fibrosis in mice, The Science of the total environment 790 (2021) 148041.

[21] S. Mehto, K.K. Jena, R. Yadav, et al., Selective autophagy of RIPosomes maintains innate immune homeostasis during bacterial infection, The EMBO journal 41 (23) (2022) e111289.
[22] I.S. Afonina, Z. Zhong, M. Karin, et al., Limiting inflammation-the negative regulation of NF-κB and the NLRP3 inflammasome, Nat. Immunol. 18 (8) (2017) 861–869.
[23] Q. Li, Y. Cheng, Z. Zhang, et al., Inhibition of ROCK ameliorates pulmonary fibrosis by suppressing M2 macrophage polarisation through phosphorylation of STAT3, Clin. Transl. Med. 12 (10) (2022) e1036.
[24] Q. Liu, Y. Bi, S. Song, et al., Exosomal miR-17-5p from human embryonic stem cells prevents pulmonary fibrosis by targeting thrombospondin-2, Stem Cell Res. Ther. 14 (1) (2023) 234.
[25] J. Yang, H. Hu, S. Zhang, et al., [Human umbilical cord mesenchymal stem cell-derived exosomes alleviate pulmonary fibrosis in mice by inhibiting epithelial-mesenchymal transition], Nan fang yi ke da xue xue bao = Journal of Southern Medical University 40 (7) (2020) 988–994.
[26] S.B. Andugulapati, K. Gourishetti, S.K. Tirunavalli, et al., Biochanin-A ameliorates pulmonary fibrosis by suppressing the TGF-β mediated EMT, myofibroblasts differentiation and collagen deposition in in vitro and in vivo systems, Phytomedicine: international journal of phytotherapy and phytopharmacology 78 (2020) 153298.
[27] J. Wang, Y. Xiang, S.X. Yang, et al., MIR99AHG inhibits EMT in pulmonary fibrosis via the miR-136-5p/USP4/ACE2 axis, J. Transl. Med. 20 (1) (2022) 426.
[28] S.Y. Kyung, D.Y. Kim, J.Y. Yoon, et al., Sulforaphane attenuates pulmonary fibrosis by inhibiting the epithelial-mesenchymal transition, BMC pharmacology & toxicology 19 (1) (2018) 13.
[29] C.M. Weng, Q. Li, K.J. Chen, et al., Bleomycin induces epithelial-to-mesenchymal transition via bFGF/PI3K/ESRP1 signaling in pulmonary fibrosis, Biosci. Rep. 40 (1) (2020).
[30] P. Spagnolo, J.A. Kropski, M.G. Jones, et al., Idiopathic pulmonary fibrosis: disease mechanisms and drug development, Pharmacology & therapeutics 222 (2021) 107798.
[31] B. JäGER, B. Seeliger, O. Terwolbeck, et al., The NLRP3-inflammasome-caspase-1 pathway is upregulated in idiopathic pulmonary fibrosis and acute exacerbations and is inducible by apoptotic A549 cells, Front. Immunol. 12 (2021) 642855.
[32] I. Lasithiotaki, E. Tsitoura, K.D. Samara, et al., NLRP3/Caspase-1 inflammasome activation is decreased in alveolar macrophages in patients with lung cancer, PLoS One 13 (10) (2018) e0205242.
[33] Z. Pu, C. Han, W. Zhang, et al., Systematic understanding of the mechanism and effects of Arctigenin attenuates inflammation in dextran sulfate sodium-induced acute colitis through suppression of NLRP3 inflammasome by SIRT1, American journal of translational research 11 (7) (2019) 3992–4009.
[34] N. Kayagaki, S. Warming, M. Lamkanfi, et al., Non-canonical inflammasome activation targets caspase-11, Nature 479 (7371) (2011) 117–121.
[35] M. Wang, X. Ye, J. Hu, et al., NOD1/RIP2 signalling enhances the microglia-driven inflammatory response and undergoes crosstalk with inflammatory cytokines to exacerbate brain damage following intracerebral haemorrhage in mice, J. Neuroinflammation 17 (1) (2020) 364.
[36] R. Caruso, N. Warner, N. Inohara, et al., NOD1 and NOD2: signaling, host defense, and inflammatory disease, Immunity 41 (6) (2014) 898–908.
[37] X. Wang, Z.F. Zhang, G.H. Zheng, et al., The inhibitory effects of purple sweet potato color on hepatic inflammation is associated with restoration of NAD^+ levels and attenuation of NLRP3 inflammasome activation in high-fat-diet-treated mice, Molecules 22 (8) (2017).
[38] Y. Zhang, J. Liang, N. Cao, et al., Coal dust nanoparticles induced pulmonary fibrosis by promoting inflammation and epithelial-mesenchymal transition via the NF-κB/NLRP3 pathway driven by IGF1/ROS-mediated AKT/GSK3β signals, Cell death discovery 8 (1) (2022) 500.
[39] X. Li, X. Yan, Y. Wang, et al., NLRP3 inflammasome inhibition attenuates silica-induced epithelial to mesenchymal transition (EMT) in human bronchial epithelial cells, Experimental cell research 362 (2) (2018) 489–497.